JOURNAL OF MATERIALS SCIENCE 22 (1987) 3771–3780

The beneficial use of composite samples in the energy-dispersive X-ray analysis of highly radioactive Nimonic PE16

P. K. ROSE, J. ROWE
Central Electricity Generating Board, Berkeley Nuclear Laboratories, Berkeley, Gloucestershire GL13 9PB, UK

A new technique for preparing 3 mm diameter disc samples for TEM is presented. It permits quantitative energy-dispersive X-ray (EDX) analysis of radioactive materials where otherwise high sample activity causes saturation of the EDX detector. The new composite sample geometry, comprising a small disc of radioactive material within an annulus of compatible unirradiated material, has up to $\sim 50\times$ reduced activity. Similar sample geometries may be used to minimize the mass of magnetic material in high-resolution TEM examinations or when samples from small diameter wires are required. Composite samples have been prepared from a Commercial Nimonic PE16 alloy containing 0.1 wt% Co after irradiation at 450° C under thermal reactor conditions. High-resolution EDX analysis in a field-emission gun STEM reveals significant irradiation-induced intergranular enrichment of nickel, silicon and phosphorus and depletion of chromium and iron. The observed changes are asymmetric with respect to the grain-boundary interface and extend over distances of 10 to 20 nm. The asymmetry may be explained by the presence of intergranular γ' phase of mixed thermal and irradiation-induced origin. A coincident irradiation-induced deterioration in stress-rupture properties may be associated with intergranular γ' and phosphorus. Future investigations should allow irradiation-induced changes in the mechanical properties of PE16 to be described in terms of coincident changes in grain-boundary microchemistry.

1. Introduction

Compositional changes in grain-boundary regions of neutron-irradiated stainless steel may be investigated using the energy-dispersive X-ray (EDX) analysis technique [1]. A small electron probe such as that available in a scanning transmission electron microscope (STEM) excites characteristic X-rays from a well-defined volume of material and the corresponding chemical composition is determined. This technique in its basic form is unsuitable for use with highly radioactive material. For instance, the spontaneous emission of characteristic manganese X-rays and cobalt γ-rays from neutron-irradiated Nimonic (Henry Wiggin, plc., UK) PE16 alloy containing > 0.1 wt % Co is so intense that the EDX detector saturates with fractional dead times of 80% or more. This feature necessitates the use of long data collection times. Normally tractable problems such as electron beam instability, sample drift and sample contamination can then become troublesome. Sample radioactivity can also give misleading major element analyses because of an overlap between the unwanted MnK_β characteristic X-ray peak and the FeK_α peak. This error increases with increasing sample radioactivity.

A new technique for preparing samples with reduced radioactivity has been developed and is presented here. To date high sample activity has hampered studies attempting to correlate compositional changes in grain-boundary regions of neutron-irradiated PE16 with mechanical property changes. The proposed technique overcomes this handicap as discussed below.

2. Definition of the problem

The nature of the problem encountered is demonstrated in Fig. 1. The spectra shown are from standard 3 mm diameter disc samples of Nimonic PE16 alloy and 20 Cr–25 Ni–Nb stainless steel irradiated at ~ 500° C under thermal reactor conditions (Figs 1a and b, respectively). They were collected in a Philips EM400T STEM fitted with a Kevex Unispec 7000 X-ray detector system. The electron beam was switched off. Thus the spectra arise because of inherent sample radioactivity and are not electron-induced. Both spectra contain characteristic MnK_α and MnK_β-X-ray peaks from transmuted iron. The PE16 spectrum has a pronounced background distribution, particularly at low energies (Fig. 1a). It was collected with long dead times, e.g. a counting time of 95 sec registered as a live time of only 18 sec. Thus the apparent count rate of 1870 c.p.s. was well in excess of the 2500 c.p.s. discrimination level of the EDX detector. Clearly electron-induced X-ray signals will appear weak against such a strong "radioactive" signal. Fig. 2 shows the "radioactive" spectrum collected from the PE16 sample when covered by a 125 μm thick tungsten

0022–2461/87 $03.00 + .12

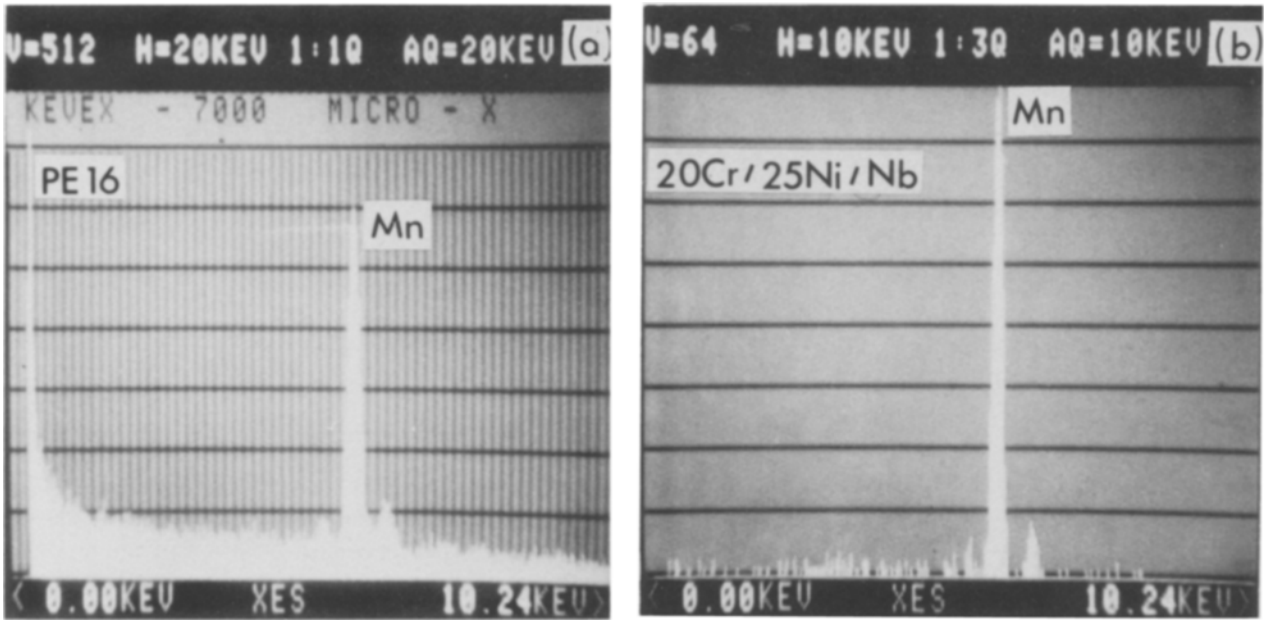

Figure 1 "Radioactive" EDX spectra from samples of neutron-irradiated (a) PE16 and (b) 20Cr–25Ni–Nb. Both were collected with the electron beam switched off. They contain characteristic manganese X-ray peaks on a background distribution.

film. The film absorbs the manganese peaks but not the background distribution. The latter is thus an instrumental effect associated with the rapid emission of high energy (1.17 and 1.33 MeV) γ-rays from transmuted cobalt. Its presence is particularly undesirable when looking for low concentrations of the low atomic number elements aluminium, silicon and phosphorus which are often involved in irradiation-induced grain-boundary phenomena (e.g. [2, 3]). Furthermore the unwanted cobalt γ-rays cannot be filtered out without loss of lower energy characteristic X-rays.

PE16 sample activity can be reduced by using smaller volumes of material. Kestel [4] has shown that it is possible to make TEM samples from very small, 0.13 mm diameter, wire specimens. His method, however, is unsuitable for the present application as it is labour-intensive and may introduce unwanted chemical effects. Consequently a new disc preparation technique has been developed. This is described below.

The conventional TEM sample geometry (Fig. 3a) comprises a central thin area suitable for examination surrounded by an unpolished rim containing up to three-quarters of the sample volume. We propose use of the composite sample geometry shown in Fig. 3b. Here a small active disc is supported by a surrounding inactive annulus. The activity reduction (R) to be achieved may be estimated by assuming that the two samples dish spherically and symmetrically during

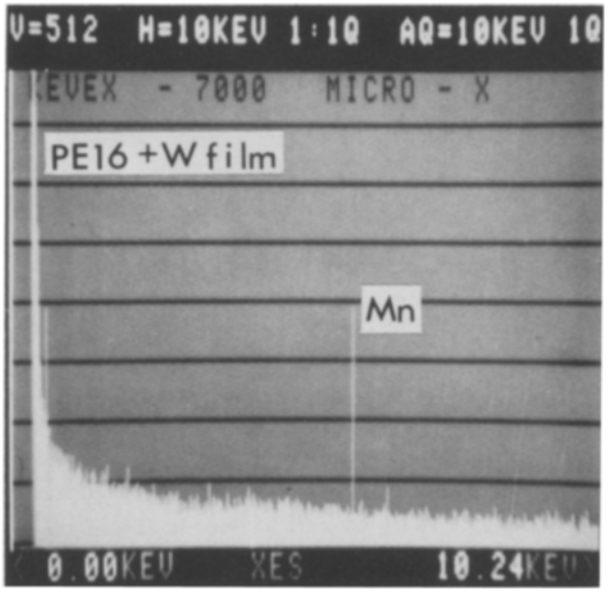

Figure 2 "Radioactive" spectrum from the PE16 sample of Fig. 1 when covered by a tungsten film. The film absorbs the manganese peaks but not the low-energy background distribution.

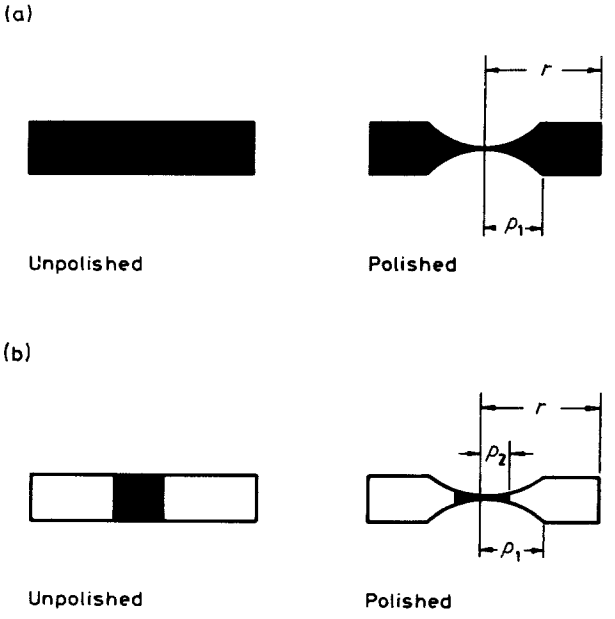

Figure 3 Schematic representations of (a) the conventional and (b) the composite sample geometry before and after preparation for EDX analysis in a STEM unit: r = disc radius, p_1 = radius of polished region, p_2 = radius of active inset region. (■) Active material, (□) non-active material.

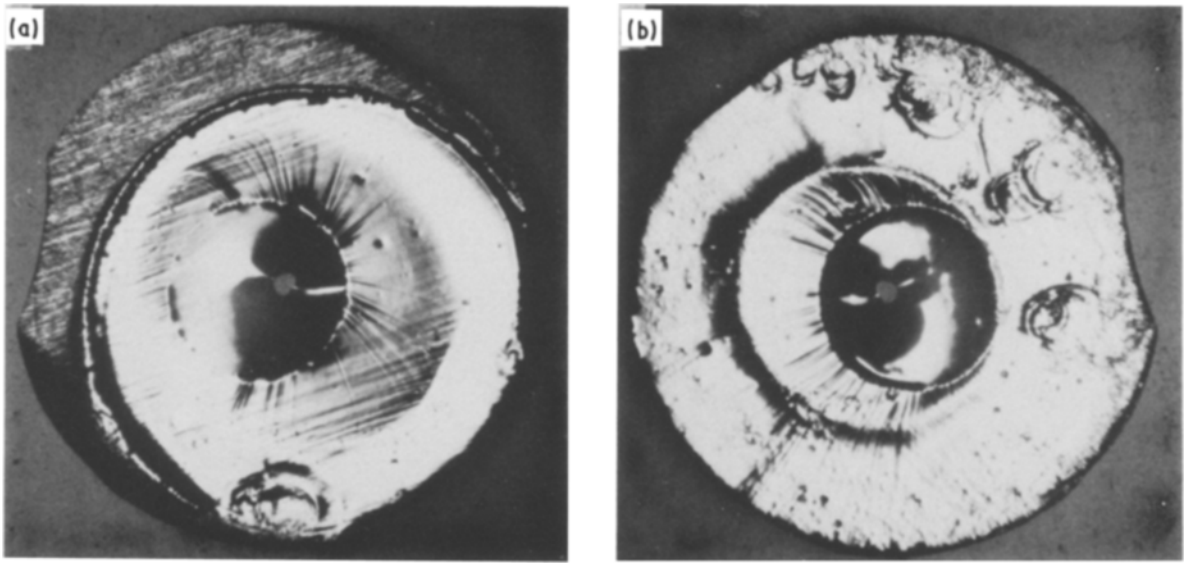

Figure 4 (a, b) Both sides of a non-active composite sample. The central perforated area contains a thin area suitable for analysis.

electropolishing. It is found that

$$R = \left(\frac{2r^2 - p_1^2}{p_1^2}\right)\left(\frac{p_1}{p_2}\right)^4$$

where r is the radius of the sample (i.e. 1.5 mm), p_1 is the radius of the central electropolished region and p_2 is the radius of the active inset region [5].

For composite samples with an active inset diameter of 1 mm, polishing over the central 2 mm diameter region, an activity reduction of $\sim 55\times$ is possible. In practice only half this value is achieved. However this is considerably greater than that obtained by preparing conventional-geometry samples from thinner or smaller-diameter discs.

3. Preparation of composite geometry samples

Active composite samples are prepared as follows. Two standard 3 mm diameter discs are punched out of the same type of material. One is irradiated and thus radioactive, the other is not. Both are about 250 μm thick. 1 mm diameter discs are punched out of each. The 1 mm active disc is pressed into the 1 mm hole of the non-active annulus. The resultant composite sample is ground down to $\sim 75\,\mu$m. The use of "glue", electroplating or otherwise, is avoided as it may introduce unwanted chemical effects. The ground composite sample is then electropolished to perforation in a Struers Tenupol (Denmark) electropolishing unit using a 5% perchloric–95% methanol electrolyte cooled to -70 to $-60°$ C as if it were a conventional, non-composite, sample.

For test purposes non-active composite samples were prepared to allow electrical continuity and/or mechanical robustness problems to be identified and remedied before using active material. Fig. 4 shows a successful example. The inset region has remained intact and has polished in unison with the outer region. One side has a larger polished area than the other, indicating that the electrolyte jets were not balanced. This has since been corrected.

Normally perforation is detected when a bright light placed behind the sample becomes visible. With composite samples this may signify junction erosion rather than perforation. Thus use of the Struers unit automatic light sensor is inappropriate. Typically discs take up to 5 min to perforate. Erosion may occur at any point in this period and so the discs must be observed throughout. Fig. 5 shows three non-active composites with various degrees of junction erosion: the first was "stopped" at first light (Fig. 5a); the second was "polished on" in a series of short bursts and inspected each time until perforation was apparent (Fig. 5b); the third was viewed off-axis so that perforation could be identified unambiguously (Fig. 5c). In all three cases the samples retained electrical continuity throughout. The two taken to perforation were examined in the TEM without supporting grids. Both contained ample thin area.

Often active sample preparation presents handling problems which are irrelevant to the case of non-active samples. The use of shielded facilities during the punching and grinding stages can lessen these [6, 7]. In addition a TV monitor can be used to observe samples remotely during the electropolishing stage. This has the added advantage of built-in magnification. Should junction erosion occur before perforation then the final stages of electropolishing may be observed by eye, knowing that exposure to radiation has at least been reduced.

4. Experimental procedure

Two composite PE16 samples were prepared. The central active regions had experienced the following conditions: solution treatment for 15 min at 1020 to 1060° C; ageing for 2.5 h at 680 to 720° C; neutron irradiation at 450° C to doses of $10.6 \times 10^{24}\,\text{nm}^{-2}$ (fast $E > 1.3$ MeV) and $9.3 \times 10^{24}\,\text{nm}^{-2}$ (thermal) under thermal reactor conditions. Unirradiated PE16 was used for the supporting annulus. One sample was examined in a conventional Philips EM400T STEM and Kevex EDX unit at Berkeley Nuclear Laboratories, the other in a high-resolution Vacuum Generators HB501 field-emission gun (FEG) STEM and

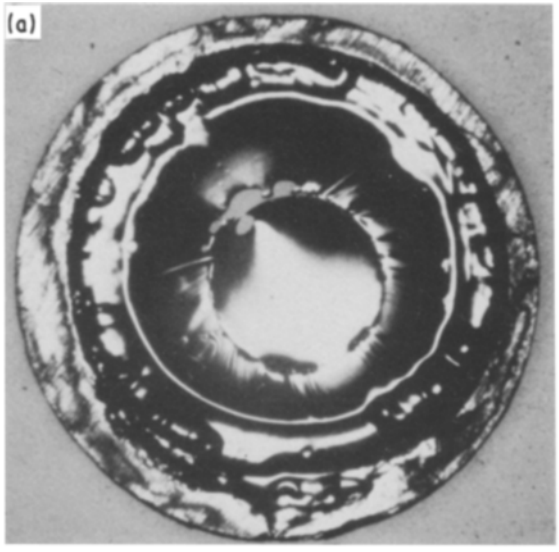

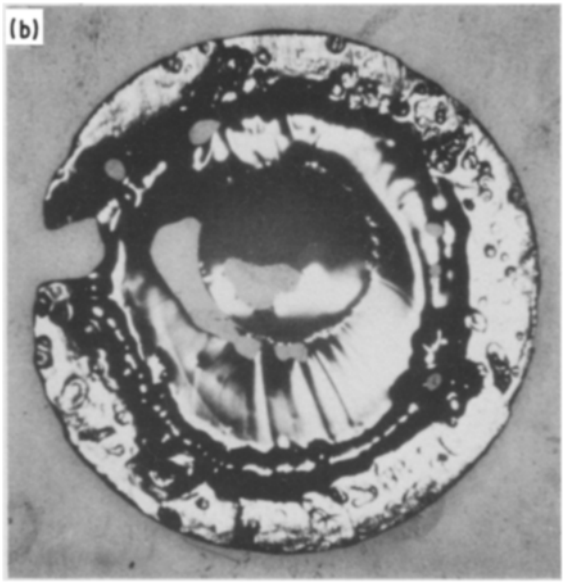

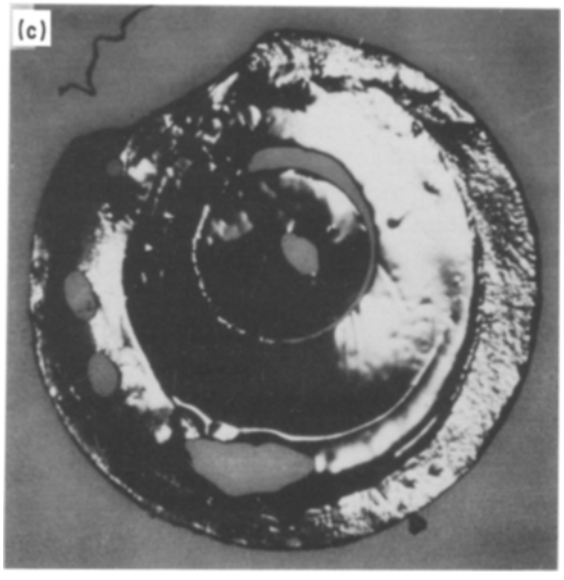

Figure 5 (a–c) Three non-active composite samples with various degrees of junction erosion. Each sample retained electrical continuity throughout. The two taken to perforation (b, c) were robust enough for examination in the STEM without the use of supporting grids.

Link Systems EDX unit at the Atomic Energy Research Establishment, Harwell. Electron probe sizes of 17 and 3 nm were used, respectively. In all cases grain boundaries were tilted parallel to the electron beam direction during examination.

5. Results

5.1. Philips EM400T/Kevex results

Fig. 6a shows an EDX spectrum obtained with the electron beam switched off. It has a low count rate (~20 c.p.s.) and no anomalous low-energy background distribution. Figs 6b and c show spectra obtained with the electron probe on and centred at "on" and "off" grain-boundary locations, respectively. Both spectra have well-defined major element chromium, iron and nickel peaks with little evidence of any "radioactive" manganese peak between the chromium and iron peaks. The minor element aluminium, silicon and phosphorus data are non-existent or poor. They require longer collection times or a brighter electron source. The latter is preferable as the combined (radioactive + electron-induced) signal count rate (typically ~400 c.p.s.) is low compared with the 2500 c.p.s. discrimination level of the EDX detector. Unfortunately a bright-source electron gun option is not available on the standard STEM at Berkeley Nuclear Laboratories.

Figs 6b and c reveal irradiation-induced changes in grain-boundary microchemistry as follows: nickel enrichment; chromium and iron depletion. However, these changes are discernible only if the electron beam is centred exactly on the boundary interface. The modified zone would appear to be narrow.

5.2. Vacuum Generators HB501/Link Systems results

The electron probe in the HB501 FEGSTEM is very small, being only ~3 nm in diameter. Normally this would result in reduced "electron-induced" signal. However the electron source is ~1000 × brighter than normal. Thus strong signals can be obtained without loss of spatial resolution. Throughout examination the composite PE16 sample was supported between copper grids. This did not present any problem as the

TABLE I Chemical compositions

Element	Composition (wt %)	
	PE16	20Cr–25Ni–Nb
C	0.06	0.065 to 0.080
Si	0.29	0.72 to 0.73
Mn	0.11	0.56 to 0.72
P	0.007	0.001 to 0.005
S	0.006	0.002 to 0.004
Cr	16.35	19.4 to 20.2
Mo	3.16	–
Ni	44.3	24.0 to 25.0
Al	1.27	0.006
B	0.004	< 0.001
Co	0.10	0.003 to 0.004
Nb	–	0.63 to 0.76
Ti	1.21	0.012 to 0.018
Zr	0.035	0.029 to 0.033
Fe	Balance	Balance

TABLE II EDX data from the composite sample investigated in the FEGSTEM at Harwell – composite profile

Position from grain-boundary interface		Normalized counts*							
		Al	Si	P	Mo	Ti	Cr	Fe	Ni
Left	15 nm	0.8	0.5	0.2	2.6	0.7	18.9	35.8	40.6
	10 nm	0.7	0.9	0.3	2.1	0.7	16.8	32.5	46.0
	5 nm	1.3	2.3	< 0.1	1.9	1.0	12.3	24.0	57.1
On	0 nm	1.2	2.7	0.7	3.9	0.9	12.2	21.2	57.1
Right	2.5 nm	0.7	1.1	0	2.4	0.5	16.3	31.3	47.7
	5 nm	0.5	0.6	< 0.1	2.4	0.6	17.4	35.1	43.3
Off	Matrix	1.0	0.6	0	3.0	1.1	18.1	33.3	42.9
Output K factors		1.15	1.00	1.02	1.56	1.03	1.07	1.15	1.23

*Counts were collected from $K\alpha$ peaks except for molybdenum where the $L\alpha$ peak was used.

copper X-ray peaks produced from the grids did not overlap any of the peaks of interest.

Fig. 7 shows spectra from "on" and "off" grain-boundary locations. The high- and low-energy regions have different full-scale deflections to display the X-ray peaks to best advantage. Typically count rates of ~2000 c.p.s. were noted. Major (chromium, iron and nickel) and minor (aluminium, silicon, phosphorus, molybdenum and titanium) element peaks are all visible in Fig. 7. The presence of the phosphorus peak is remarkable as the sample only contains 70 p.p.m. P (Table I). Nickel enrichment and depletion of chromium and iron are apparent as before (Section 5.1) with evidence of silicon and phosphorus enrichment also.

Fig. 8 shows some of the spectra obtained in a grain-boundary profile sequence. The corresponding X-ray data (Table II) are plotted as weight percentages in Fig. 9 after scaling by the appropriate Cliff-Lorimer K correction factors. The "off" boundary compositions agree well with the chemical specification showing that the K correction factors used are reasonable. Individual elemental profiles are asymmetric. They extend ~15 nm to the left but only ~5 nm to the right of the boundary interface (Fig. 9). Coincidentally, the left-hand side exhibited black contrast when imaged in bright-field conditions (Fig. 8d). Thus the asymmetry may be due to precipitation. The strong nickel and silicon signals suggest γ' phase. Subtraction of precipitate contributions from the left-hand spectra would enhance the relative contributions from non-precipitate elements such as chromium and iron. In turn their profiles would look more symmetrical. Unfortunately this explanation could not be investigated directly. Firstly the chance of detecting weak γ' superlattice reflections from small features is minimal. Secondly, there was not sufficient time available to obtain composition profiles from both "black" and "clear" boundary interfaces. A quick test was performed as follows. Using a working magnification of 2×10^6 the electron probe was scanned across two separate rectangular areas. The first, centred on a "black" interface, gave Spectrum I (segregation + precipitation). The second, centred on a "clear" interface, gave Spectrum II (segregation only). Spectrum II was scaled to make its chromium counts equal to those of Spectrum I. Assuming the precipitate to be γ' and chromium-free [8], the difference between these spectra was processed to give the following precipitate composition (at %): Al 5.7, Si 10.9, P 2.5, Mo 0.9, Ti 3.6, Cr 0, Fe 3.9 and Ni 72.5. Considering the main γ' forming elements [8] this reduces to Al 6.1, Si 11.8, Ti 3.9 and Ni 78.2, consistent with Ni_3(Al, Si, Ti) or γ' phase. Developing this idea further,

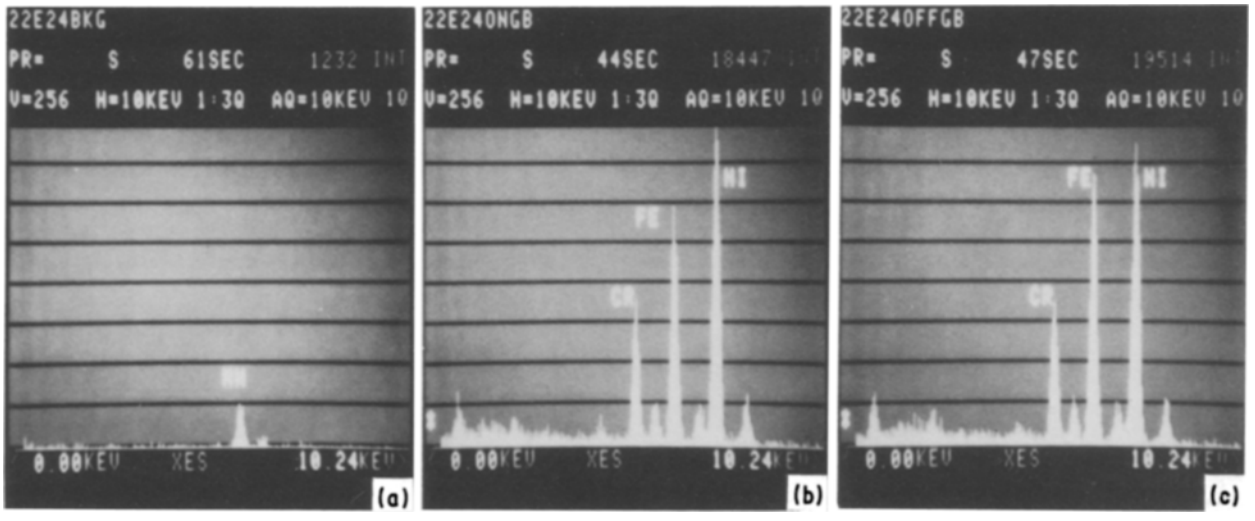

Figure 6 (a) "Radioactive" spectrum collected from a composite PE16 sample. Note that there is no low-energy background distribution. (b, c) "Electron-induced" spectra collected from "on" and "off" grain-boundary locations, spectra (a) to (c) were obtained in a standard STEM.

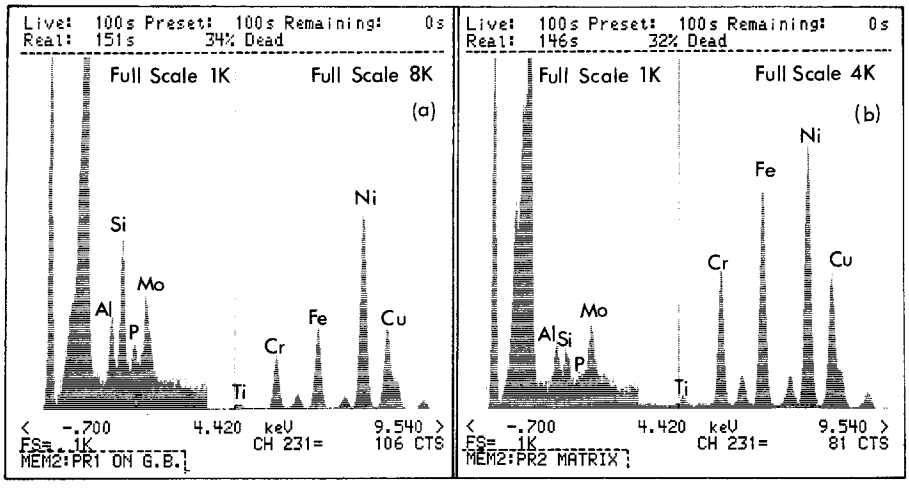

Figure 7 "Electron-induced" spectra collected from (a) "on" and (b) "off" grain-boundary locations. They were obtained in a FEGSTEM. Comparison with Fig. 6 shows that they contain considerably more microchemical information.

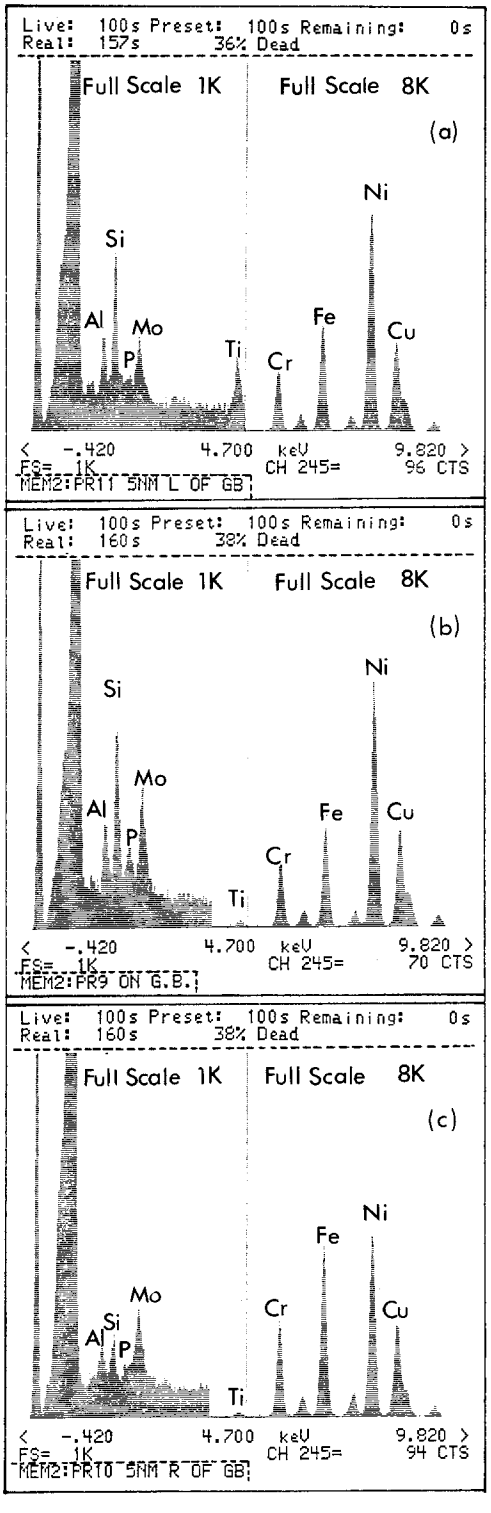

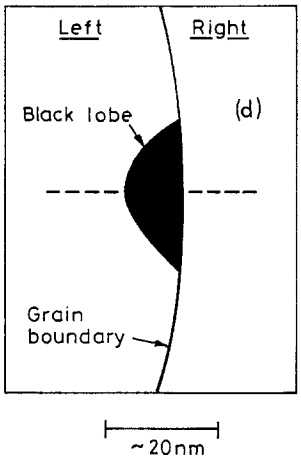

Figure 8 Spectra collected with the electron probe centred (a) 5 nm to the left, (b) on and (c) 5 nm to the right of a grain-boundary interface, (d) schematic representation of the region investigated. The dashed line connects points from which the spectra were collected.

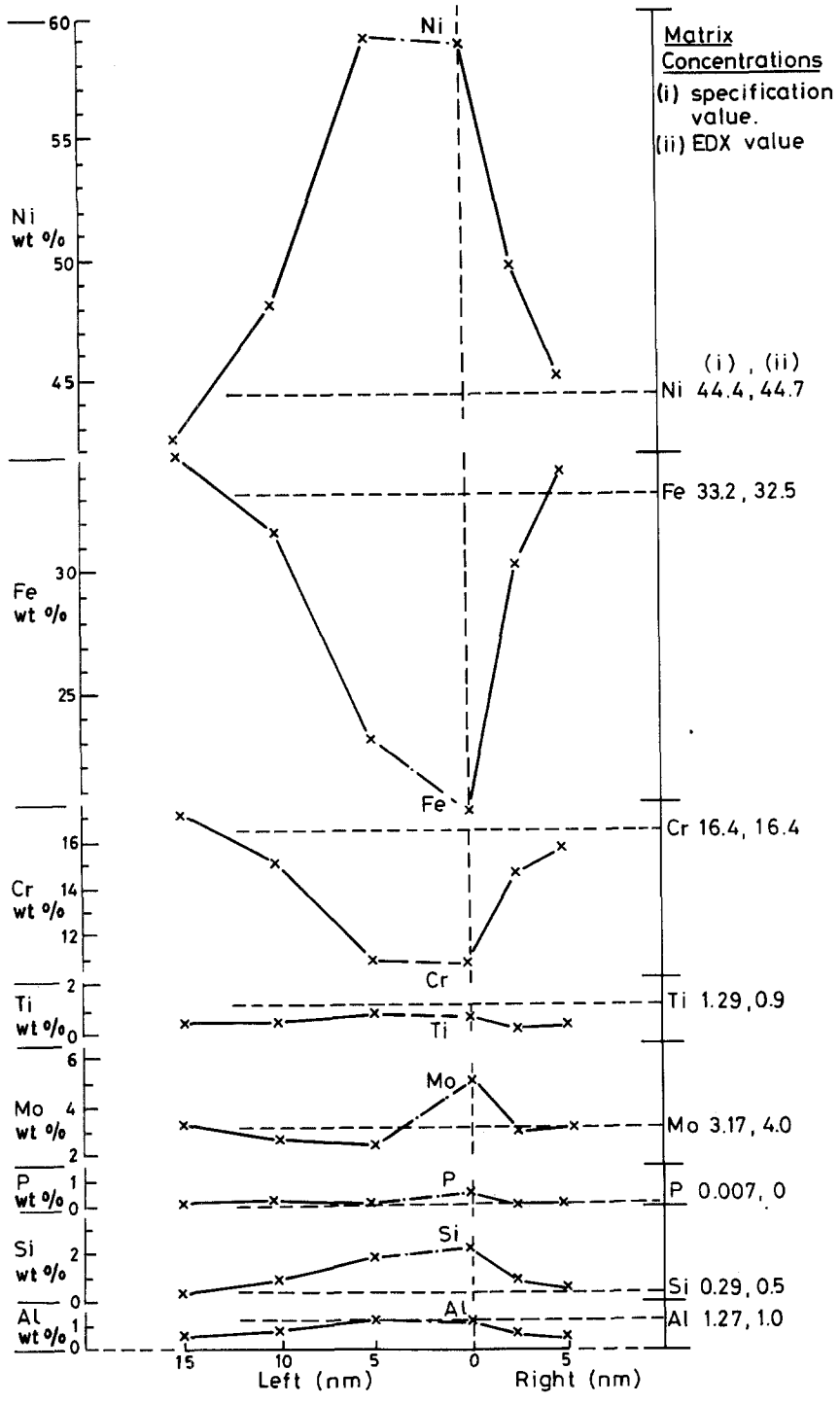

Figure 9 Chemical profiles obtained across the grain-boundary interface shown in Fig. 8d. Matrix concentrations based on the chemical specification of Table I (indicated by horizontal dashed lines) and the EDX analysis of Fig. 7b are given for reference. The profiles are asymmetric with respect to the boundary interface.

precipitate contributions were removed from the profiles of Fig. 9. Removal was based on the nickel counts as follows. The difference between the 5 nm left (segregation + precipitation) and the 5 nm right (segregation) nickel percentage counts was taken to represent the precipitate contribution to the observed nickel counts at the 5 nm left position. Similar assumptions were made for the 10 and 15 nm left data by reference to "off" boundary data. In turn precipitate contributions of 24%, 6% and 0% were determined for the 5, 10 and 15 nm positions, respectively. A nominal 12% (i.e. 1/2 × 24%) contribution was assumed for the 0 nm or "on" position as it obviously contains precipitate information in its left half. Counts for other precipitate elements were assigned in proportion to the precipitate spectrum counts determined above. Subtraction of the appropriate precipitate signals gives the normalized profiles of Fig. 10. Not surprisingly the new nickel profile looks more symmetrical than in Fig. 9. More significantly the other precipitate (silicon, aluminium) and non-precipitate (chromium, iron) elemental profiles all look more symmetrical. These observations confirm that the presence of intergranular γ' phase is reasonable.

Fig. 11 shows a spectrum collected from an intergranular precipitate thought to be one of the 20 to 25 nm diameter irradiation-induced (nickel–silicon-rich) precipitates reported elsewhere [9]. The precipitate was in a thin area of matrix to minimize any matrix contribution to the observed EDX signal. Using a subtraction process similar to that above, the following precipitate composition (at %) was determined: Al 4.5, Si 22.1, P 0.1, Ti 1.2, Fe 2.1 and Ni 70.0. This reduces to Al 4.6, Si 22.6, Ti 1.2 and

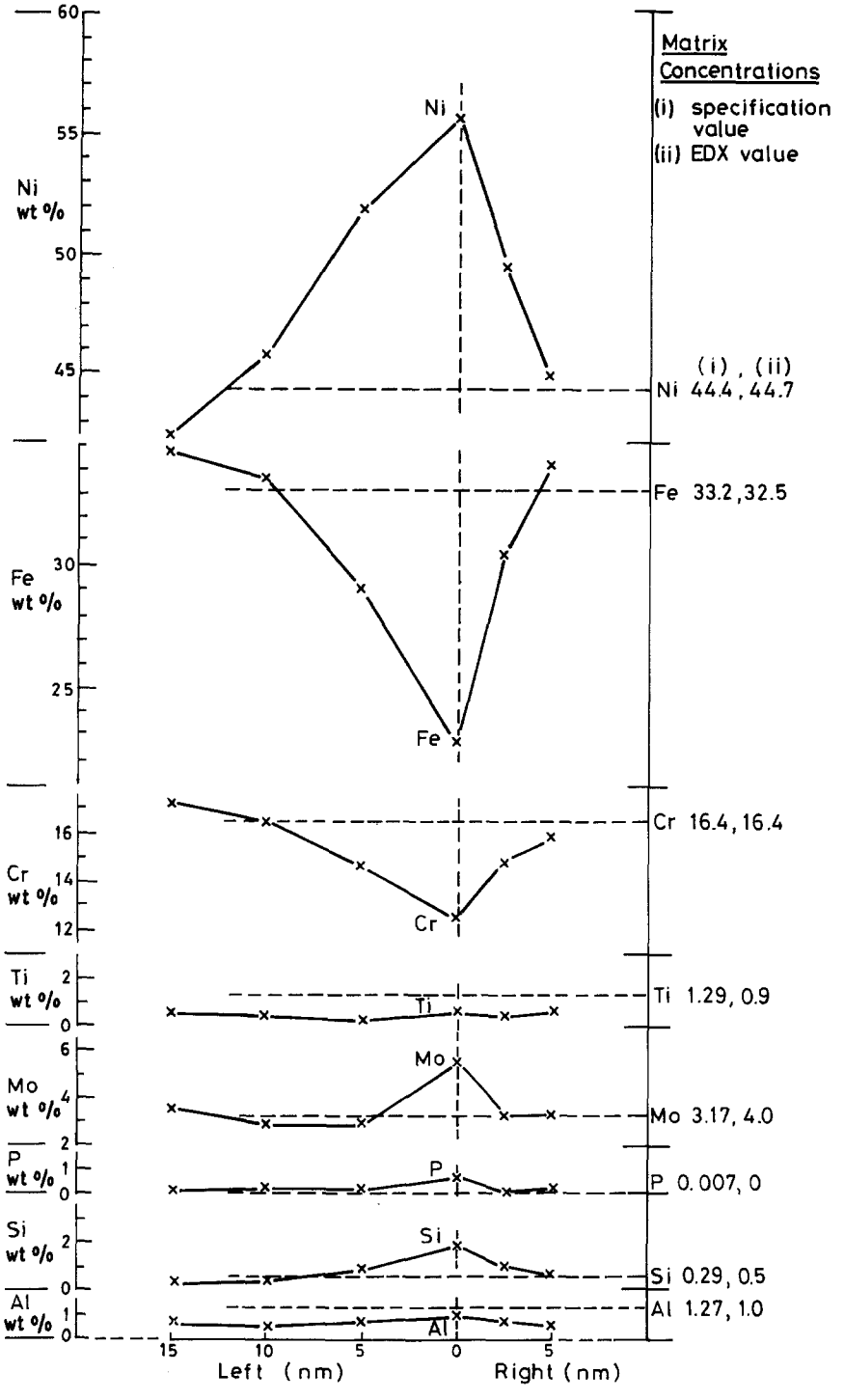

Figure 10 The profiles of Fig. 9 replotted after subtraction of an assumed γ' precipitate contribution to spectra from the left-hand side of the boundary interface (see text). Improved symmetry is noted.

Ni 71.6. The intragranular precipitate like the proposed intergranular one is again consistent with $Ni_3(Ti, Al, Si)$ or γ' phase. Its composition is different, however. The large silicon content suggests an essentially irradiation-induced phase, while the intergranular phase may be partly thermally-produced.

6. Discussion

Improvements in both major (chromium, iron, nickel) and minor (aluminium, silicon, phosphorus, titanium, molybdenum) element information is noted when using reduced-activity, composite geometry, samples. Generally $K\alpha$ X-ray peaks are used in EDX analysis, except for molybdenum where the $L\alpha$ peak is used. Overlap between the "radioactive" Mn$K\beta$ peak and the Fe$K\alpha$ peak can make the latter appear stronger than it really is. In turn the iron concentration is overestimated and the other elemental concentrations are underestimated in proportion to their relative concentrations. This is a major-element effect which increases with sample radioactivity. It is not evident in the present investigation as the composite sample "off" boundary compositions of Fig. 9 show good agreement with the chemical specification. Minor-element information can be affected by high sample activity also (Section 2). Previously EDX data has been reported for conventional geometry samples of PE16 material containing only 0.03 wt % Co [10], but only limited silicon data are available for PE16 material with 0.1 wt % cobalt [11]. The composite sample approach adopted here allows meaningful aluminium, phosphorus, titanium and molybdenum data to be obtained in addition.

The results obtained in the FEGSTEM experiment

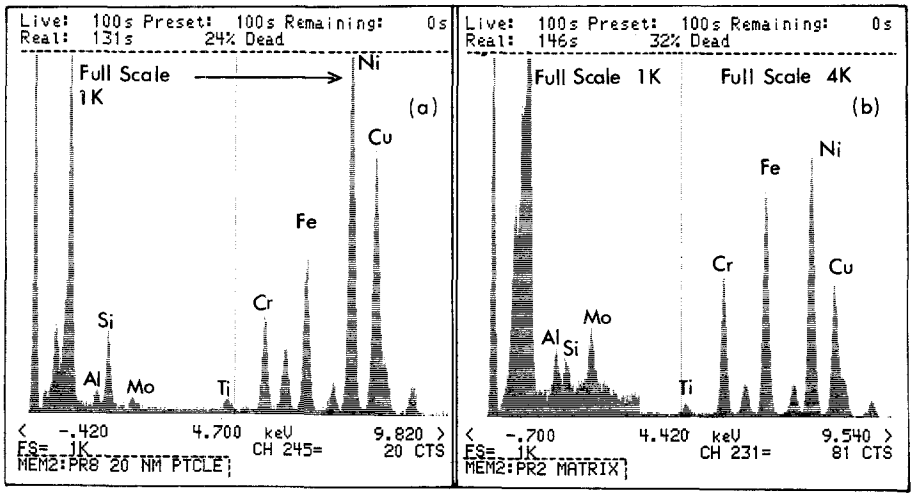

Figure 11 EDX spectra from (a) an intragranular irradiation-induced particle contained in a thin region of matrix and (b) a matrix region. The precipitate is rich in nickel, silicon and aluminium.

indicate that the width of the segregation effect after irradiation at 450° C is narrow, either 10 or 20 nm, depending on whether the observed asymmetry in Fig. 9 is genuine or due to γ' precipitation. In either case the effect requires high spatial resolution for detection. This explains why it was difficult to detect in the conventional STEM unit using a 17 nm diameter electron probe.

The boundary profiles of Fig. 9 are asymmetric with respect to the grain-boundary interface. This may be explained by the presence of γ' phase to one side of the boundary (Section 5.2). Norris *et al.* [1] observe a similar asymmetry in neutron-irradiated 20Cr–25Ni–Nb which they suggest arises because of boundary migration. If migration occurs during prior heat-treatment then the material retains some memory of it during irradiation. Alternatively it occurs during irradiation at temperatures below 418° C. The precipitate explanation advanced here seems more plausible.

It is known that the stress-rupture properties of the PE16 material investigated here deteriorate during irradiation and that they may be recovered during post-irradiation annealing at 600° C [9]. The irradiation-induced effect involved is thus thermally unstable. Interestingly the proposed intergranular γ' phase is silicon-rich (6.1 at % Al, 11.8 at % Si, 3.9 at % Ti, 78.2 at % Ni) and should not precipitate in alloys containing less than 5 to 6 wt % Si (e.g. [12]). This suggests that it is, at least in part, irradiation-induced. Furthermore, irradiation-induced γ' is known to be thermally unstable at 600° C [9]. Thus the proposed intergranular phase is a candidate property for correlation with the stress-rupture effect. Yang [10] notes a similar conclusion. His PE16 material was unaged prior to irradiation and contained no thermal γ'. Extensive precipitation occurred during irradiation and the high resolution of the FEGSTEM, essential to the present investigation, was not required during examination.

The present data suggest that the interfacial phosphorus concentration may be enhanced by up to 100 ×. Auger spectroscopy studies reveal the existence of high phosphorus levels at fracture surfaces in PE16 [13]. Thus phosphorus may be another candidate for correlation with the observed stress-rupture behaviour.

The composite sample preparation technique may be applied to other situations where some bulk property of the material needs to be reduced or where only limited quantities of material, such as small-diameter wires, are available. Magnetic material can be difficult to examine in the STEM if its internal magnetic field is strong enough to interfere with the magnetic field of the lens systems or alternatively to deflect electrons as they pass through the sample. Composite samples could be made from 1 mm diameter magnetic material supported by a non-magnetic annulus. The final sample should be about 25 × less magnetic than its conventional counterpart.

7. Concluding summary

Good major and minor element information may be obtained from radioactive material using the EDX analysis technique provided that composite geometry samples are investigated in a FEGSTEM facility. The new sample preparation technique developed for the present study may be used in other experiments where sample magnetism or small available mass, rather than radioactivity, is a problem. The results obtained show that grain-boundary enrichment of nickel, silicon and phosphorus and depletion of chromium and iron occurs over distances of 10 to 20 nm following the thermal neutron irradiation of Nimonic PE16 alloy at 450° C. Asymmetry in the observed elemental profiles is attributed to intergranular γ' of mixed thermal and irradiation-induced origin. The latter is thermally unstable and a candidate property for correlation with the known irradiation-induced deterioration in stress-rupture properties of the material investigated. Correlation with phosphorus is also possible. The intergranular phosphorus content is found to be up to 100 × greater than the bulk composition value.

Acknowledgements

This paper is published by permission of the Central Electricity Generating Board. The authors are grateful to the UKAEA for use of the FEGSTEM facility at Harwell and to Messrs R. M. Boothby, S. Dumbill and I. A. Vatter for assistance and discussion.

References

1. D. I. R. NORRIS, C. BAKER and J. M. TITCHMARSH, in Proceedings of Symposium on Radiation-induced Sensitisation of Stainless Steels, Berkeley Nuclear Laboratories, September 1986, edited by D. I. R. Norris (Central Electricity Generating Board, U.K., 1987) p. 86.
2. E. H. LEE, P. J. MAZIASZ and A. F. ROWCLIFFE, in Proceedings of Conference on Phase Stability During Irradiation, Pittsburg, October 1980, edited by J. R. Holland, L. K. Mansur and D. I. Potter (Metals Society, AIME, 1980) p. 191.
3. T. M. WILLIAMS, J. M. TITCHMARSH and D. R. ARKELL, UKAEA Report No. AERE-R-10387 (1981).
4. B. J. KESTEL, Argonne National Laboratory Report No. ANL-80-120 (1981).
5. P. K. ROSE and J. ROWE, CEGB Report No. TPRD/B/0808/R86 (1986).
6. J. ROWE, P. K. MADDEN and V. M. CALLEN, CEGB Report No. RD/B/N4747 (1980).
7. V. M. CALLEN and E. J. COOPER, Private communication (1980).
8. C. G. WINDSOR, V. S. RAINEY, P. K. ROSE and V. M. CALLEN, *J. Phys. F: Met. Phys.* **14** (1984) 1771.
9. P. K. ROSE and V. M. CALLEN, in Proceedings of Conference on Nuclear Fuel Performance, Stratford-on-Avon, March 1985, edited by D. O. Pickman (British Nuclear Energy Society, London, 1985) p. 401.
10. W. J. S. YANG, *J. Nucl. Mater.* **108/109** (1982) 339.
11. R. M. BOOTHBY and S. DUMBILL, Private communication (1986).
12. P. K. RASTOGI and A. J. ARDELL, *Acta. Metall.* **19** (1971) 321.
13. P. S. SKLAD, R. E. CLAUSING and E. E. BLOOM, in Symposium on Irradiation Effects in the Microstructure and Properties of Metals, St. Louis, May 1976, edited by J. B. Wheeler, H. M. Hoersch and E. J. McGlinchey (ASTM STP 611: American Society for Testing and Materials, Philadelphia, Pennsylvania, 1976) p. 139.

Received 9 January
and accepted 1 April 1987